

Gallium-Doped Silicon for High-Efficiency Commercial Passivated Emitter and Rear Solar Cells

Nicholas E. Grant,* Pietro P. Altermatt, Tim Niewelt, Regina Post, Wolfram Kwapil, Martin C. Schubert, and John D. Murphy*

Czochralski-grown gallium-doped silicon wafers are now a mainstream substrate for commercial passivated emitter and rear cell (PERC) devices and allow retention of established processes while offering enhanced cell stability. We have assessed the carrier lifetime potential of such Czochralski-grown wafers in dependence of resistivity, finding effective lifetimes well into the millisecond region without any gettering or hydrogenation processing, thus demonstrating one advantage over boron-doped silicon. Second, the stability of gallium-doped PERC cells are monitored under illumination (>3000 h in some cases) and anomalous behavior is detected. While some cells are stable, others exhibit a degradation then recovery, reminiscent of light and elevated temperature-induced degradation (LeTID) observed in other silicon materials. Surprisingly, cells from one ingot exhibit LeTID-like behavior when annealed at 300 °C but near stability when not annealed, but, for another ingot, the opposite is observed. Moreover, a stabilization process typically used to mitigate boron–oxygen degradation does not influence any cells that are studied. Secondary-ion mass spectrometry of the PERC cells reveals significant concentrations of unintentionally incorporated boron in some cases. Nevertheless, even in the absence of mitigating light-induced degradation, Ga-doped silicon is still more stable than unstabilized B-doped silicon under illumination.

light-induced degradation (LID), the inclusion of this additional processing step is unattractive because it is not well controlled, and thus the final regeneration state of the solar cell is often not known. Recently, gallium-doped silicon has taken a substantial share of monocrystalline PERC production,^[4] as it is widely reported to have stable excess carrier lifetime (henceforth just “lifetime”) under illumination^[5,6] without requiring major changes to processing conditions established for boron-doped substrates.


Published research into lifetime issues associated with gallium-doped silicon is relatively limited. Although relatively well-understood lifetime changes occur in gallium-doped silicon when it is deliberately contaminated with iron^[7–11] or copper,^[12] it is not clear how important these effects are in modern commercial gallium-doped Cz wafers. Given gallium-doped silicon’s relatively recent transition to commercial importance, research to understand its carrier lifetime limitations is a key research focus.

At a device level, older studies report the efficiencies of gallium-doped monocrystalline cells are stable under illumination.^[5,6] Our recent work has however shown that dark-annealed Ga-doped PERC cells can degrade when exposed to light—albeit on a much smaller degradation scale than B-doped PERC—and this degradation occurs due to a reduction in bulk lifetime.^[13] We found the level of degradation in unannealed gallium-doped PERC devices was fairly small, but the magnitude of the degradation was larger after dark annealing, with the magnitude of the degradation dependent

1. Introduction

The majority of commercial solar cells are now fabricated from Czochralski (Cz) silicon wafers, with most using *p*-type substrates and a passivated emitter and rear cell (PERC) design. Historically substrates have been boron doped, but it is well documented that boron–oxygen-related recombination centers form under illumination^[1] and these degrade cell efficiencies. Although regeneration processes^[2,3] can eliminate this

Dr. N. E. Grant, Prof. J. D. Murphy
School of Engineering
University of Warwick
Coventry CV4 7AL, UK
E-mail: nicholas.e.grant@warwick.ac.uk; john.d.murphy@warwick.ac.uk

 The ORCID identification number(s) for the author(s) of this article can be found under <https://doi.org/10.1002/solr.202000754>.

© 2021 The Authors. Solar RRL published by Wiley-VCH GmbH. This is an open access article under the terms of the Creative Commons Attribution License, which permits use, distribution and reproduction in any medium, provided the original work is properly cited.

DOI: 10.1002/solr.202000754

Dr. P. P. Altermatt
Trina Solar Limited
State Key Laboratory for PV Science and Technology (SKL)
Changzhou 213031, China

Dr. T. Niewelt, R. Post, Dr. W. Kwapil, Dr. M. C. Schubert
Fraunhofer Institute for Solar Energy Systems ISE
Heidenhofstraße 2, 79110 Freiburg, Germany

Dr. T. Niewelt, R. Post, Dr. W. Kwapil
Laboratory for Photovoltaic Energy Conversion
Department of Sustainable Systems Engineering (INATECH)
University of Freiburg
Emmy-Noether-Str. 2, 79110 Freiburg, Germany

on temperature in the 200–300 °C range. Our data had characteristics in common with light and elevated temperature-induced degradation (LeTID), which has been found to occur in many types of silicon substrates^[14] including boron-doped float-zone silicon (FZ-Si),^[15] multicrystalline silicon (mc-Si),^[16–18] and Czochralski (Cz) silicon, which is *p*-type^[19] or *n*-type.^[20,21] There are also now indications that signs of LeTID occur in Ga-doped Cz silicon substrates.^[22,23] Establishing why so many different silicon material and device types undergo apparently similar degradation and recovery is an open question.

This article addresses two key areas which demonstrate why Ga-doped Cz silicon is superior to boron-doped Cz silicon, namely i) the effective lifetime potential of the Ga-doped material without high temperature gettering or hydrogenation, and ii) the inherent stability of Ga-doped silicon. Nevertheless, the performance of gallium-doped silicon for commercial silicon solar cells can still be improved, and this article highlights where advancements can be made.

2. Results and Discussion

2.1. Lifetime Potential of Ga-Doped Silicon Wafers

The lifetime potential of gallium-doped Cz silicon is yet to be fully understood or demonstrated. Although the longevity and stability of the material is relatively well documented, the bulk lifetime needs to be equivalent to, or better than, boron-doped silicon, otherwise its use will lower cell efficiency. In this work, we measure the lifetime of “as-received” Ga-doped Cz silicon wafers and compare this with the lifetime of boron-doped silicon after the latter has undergone additional gettering and boron-oxygen stabilization treatments (e.g., regeneration). The results are shown in **Figure 1**.

Figure 1a shows the effective lifetime (orange circles) at an excess carrier density $\Delta n = 0.1 \times N_A$ (where N_A is the net acceptor concentration) as a function of resistivity for Ga-doped

Cz silicon wafers passivated with Al_2O_3 , in accordance with measurement methods described in the Experimental Section. For comparison, the blue dashed line is the lifetime limit of boron-doped silicon wafers once they have been getterted (e.g., 1 h 850 °C phosphorus diffusion to remove metal impurities) and are thus solely limited by the boron-oxygen defect.^[24] However, this boron-oxygen limit can be overcome by subjecting boron-doped silicon wafers to a very important boron-oxygen stabilization treatment (e.g., 100 mW cm^{-2} illumination at 150–250 °C or by high current injection at elevated temperature).^[2,3,25] When this stabilization treatment is carried out post getterting, or after cell manufacturing, a substantial increase in the lifetime of boron-doped Cz silicon occurs, as represented by the parameterization developed by Walter et al.^[25] (black solid line) in Figure 1a. Therefore, comparing our data (orange circles) to the parameterization of Walter et al. we see that “as-received” Ga-doped Cz silicon can achieve comparable lifetimes to treated boron-doped Cz silicon, thus making it clear that Ga-doped Cz silicon does have a high lifetime potential. Additional getterting and fast firing processes, as commonly carried out in the production of PERC solar cells, are likely to further enhance its lifetime—potentially beyond realistic potentials of boron-doped Cz silicon.

Turning our attention to Figure 1b, it can be seen from the injection-dependent lifetime curves that one or more defects are limiting the lifetime, as we see a reduction in lifetime as the injection level Δn decreases. We do not attribute this to surface effects (e.g., depletion region recombination), as the deposited atomic layer deposition (ALD) Al_2O_3 film possesses a very high negative charge,^[26] thereby forming an accumulation of majority carriers at the surface of *p*-type silicon, and thus would result in a flattening of the lifetime curve at lower injection levels (i.e., $<10^{15} \text{ cm}^{-3}$). Thus, we conclude that the unprocessed gallium-doped silicon wafers investigated in our study contain bulk defects which are limiting the lifetime. **Figure 2a** shows this observation.

Effective lifetimes, such as those shown in Figure 1b, are determined by a combination of intrinsic and different extrinsic

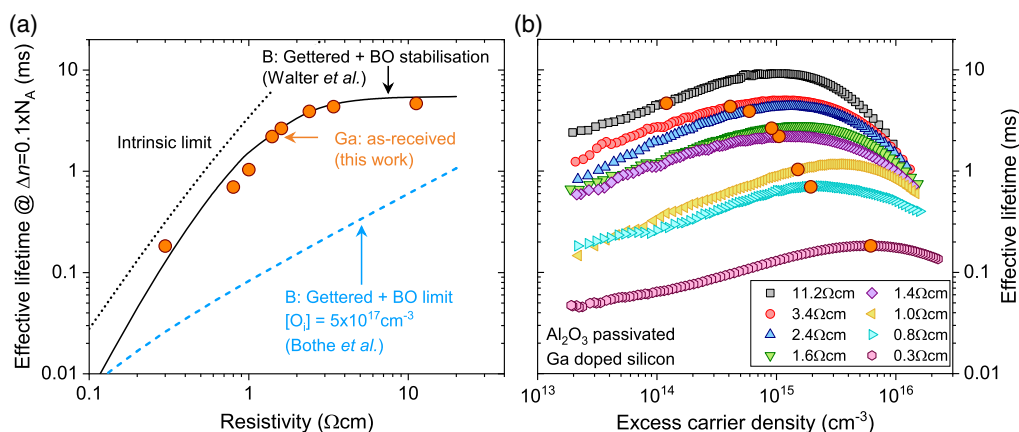


Figure 1. a) Effective lifetime at an excess carrier density $\Delta n = 0.1 \times N_A$ as a function of resistivity for Al_2O_3 passivated Ga-doped Cz silicon wafers (orange circles). The blue dashed line corresponds to the expected boron-oxygen degraded lifetime limit of getterted wafers.^[24] The black solid line corresponds to the lifetime limit of boron-doped Cz silicon once it has been getterted, and has undergone an boron-oxygen stabilization step.^[25] The black dotted line is the intrinsic limit.^[27] b) The corresponding injection-dependent effective lifetime curves for the data presented in (a) for as-received Ga-doped silicon. The orange circles in (b) are the same data set presented in (a).

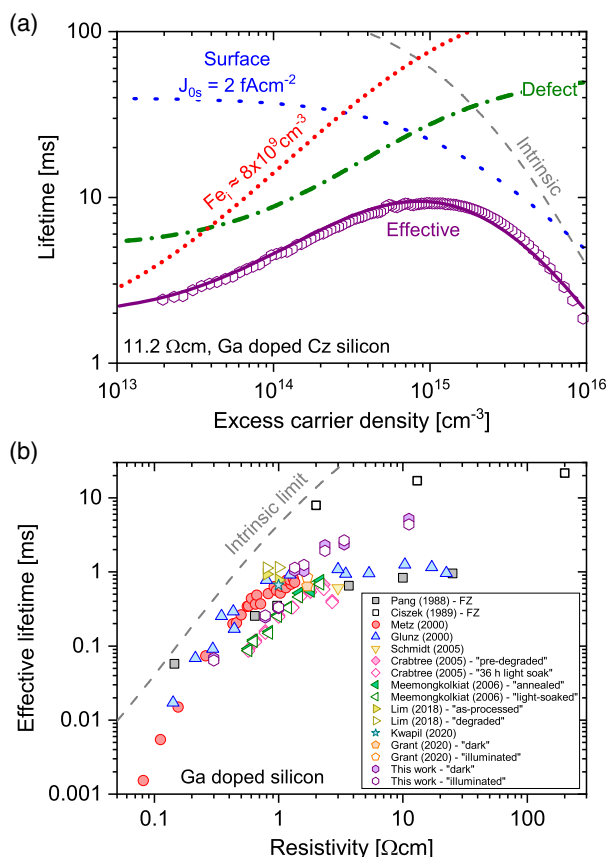


Figure 2. a) Analysis of injection-dependent lifetime data for Al_2O_3 passivated $11.2\ \Omega\text{cm}$ Ga-doped Cz silicon. We use knowledge of the surface recombination and intrinsic lifetime to estimate the bulk lifetime, as discussed in the text. b) Effective lifetime versus resistivity for gallium-doped monocrystalline silicon. The plot compares our data from Figure 1b at an excess carrier density of $1 \times 10^{14}\ \text{cm}^{-3}$ with those from the literature.^[6,7,13,22,29–34] Some studies reported lifetimes after different treatments, with open symbols generally used for illuminated samples. The intrinsic lifetime limit at an excess carrier density of $1 \times 10^{14}\ \text{cm}^{-3}$ ^[27] is also shown. Limitations of this plot arise from the lack of detail provided in previous publications, as discussed in the text.

mechanisms and we highlight this with the example in Figure 2a for the highest lifetime samples ($11.2\ \Omega\text{cm}$). For Figure 2a, we calculate the lifetime components by accounting for the surface recombination (taking a surface saturation current density, J_{0s} , as $2\ \text{fAcm}^{-2}$ for each surface as guided by our experimental data) and the intrinsic lifetime from Richter et al.^[27] Fitting the data with Shockley–Read–Hall (SRH) theory requires the existence of two defects: i) a deep-level bulk defect, which we approximate to have an energy level at midgap ($E_c - 0.56\ \text{eV}$) and SRH electron lifetime parameter of $\tau_{n0} = 5\ \text{ms}$ and a SRH hole lifetime parameter of $\tau_{p0} = 50\ \text{ms}$; and ii) another deep-level defect ($E_c - 0.79\ \text{eV}$) corresponding to interstitial iron (Fe_i) with $\tau_{n0} = 1.4\ \text{ms}$ and $\tau_{p0} = 165\ \text{ms}$.^[28] Noting that our Ga-doped silicon samples have not undergone a high temperature gettering process, it is expected that some of the injection dependence can be attributed to metal impurities, most likely iron. Our experiments on this sample set have indicated the presence of interstitial Fe

contamination, as we observe an increase in lifetime after illumination (for 20 s at 1 Sun), followed by a slow decay in lifetime when stored in the dark for up to 72 h. This is consistent with the reformation time scales of FeB and FeGa pairs.^[1,9–11] While we have indications that FeGa pairs are forming recombination centers in our Ga-doped silicon samples, it is difficult to determine the concentration of iron from traditional lifetime measurement techniques (despite our best efforts), as the FeGa pairs apparently never fully dissociate under illumination at room temperature. If we do assume 100% FeGa dissociation post illumination (for 20 s at 1 Sun), our best estimate of the iron concentration is of order $10^9\ \text{cm}^{-3}$ and is consistent with our findings in Figure 2a. Regardless of knowing a precise value for the interstitial iron concentration, the injection dependence in Figure 2a cannot be fully described by low levels of iron contamination alone and thus required another defect to fit the experimental lifetime curve. Therefore, although metal impurities such as Fe_i can be getterd during cell fabrication (e.g., during emitter formation), an unidentified defect like that shown in Figure 2a may not be annihilated or getterd in the same way, and thus attention should be paid to mitigating this defect, as it will impact the fill factor (FF) of the cell's IV curve by lowering the voltage at maximum power point (V_{mpp}), and thus limit the solar cell efficiency.

To assess the lifetime potential of Ga-doped silicon in a much broader sense, we compare our effective lifetime data at $10^{14}\ \text{cm}^{-3}$ injection to those in the literature for samples which have not intentionally been contaminated^[6,7,13,22,29–34] in Figure 2b. The intrinsic lifetime limit from Richter et al.^[27] at $10^{14}\ \text{cm}^{-3}$ injection is also plotted. We note that the lifetime, at least in our sample set, is predominantly limited by a bulk defect at this injection level. This is evident from Figure 2a and thus the lifetime values in Figure 2b should be considered as a lower limit to Ga-doped silicon's achievable bulk lifetime. This injection level also approximately corresponds to maximum power point (MPP) conditions for a state-of-the-art PERC cell guided by parameters in the literature.^[35,36] Making a completely accurate comparison is challenging because some publications provide insufficient detail, with injection conditions, surface passivation, sample type (wafer or block), and any pretreatment (thermal or optical) not always stated or clear. We assume that the other studies also use relatively low injection when not stated explicitly. Another difference between the studies is the choice of surface passivation with Pang et al. using liquid HF ,^[29] Metz et al.^[31] and Schmidt and Macdonald^[7] using SiN_x , Lim et al. and Kwapił et al. using $\text{Al}_2\text{O}_3\text{-SiN}_x$ stacks,^[22,34] Meemongkolkiat et al. using iodine-methanol,^[6] and Grant et al. using ALD Al_2O_3 .^[13] As discussed previously,^[37] surface passivation processes can affect effective lifetimes not just by the extent to which they modify surface recombination, but also because they can play a role in impurity gettering and bulk hydrogenation. Our high-quality passivation may explain why for relatively high resistivity samples, we measure higher values than Glunz et al.^[32] who do not state a passivation scheme. We also note that Pang et al. and Ciszek et al. used gallium-doped FZ-Si,^[29,30] whereas all other studies presumably used Cz silicon or magnetic Cz silicon, and that the material used for the results shown in Figure 1 was grown by a different manufacturer to the material used for our previous lifetime study.^[13]

While we acknowledge the limitations of the comparisons made in Figure 2b, the general trends it contains are highly significant for the use of gallium-doped silicon in solar cells. First, the effective lifetime in Ga-doped silicon from a range of suppliers is as strongly resistivity dependent as is observed for phosphorus and boron-doped ingots.^[4] Results in Figure 1 of this article show the trend known from earlier studies (such as Metz et al.^[31]) extends to more resistive samples, with lifetimes > 5 ms measured at $1 \times 10^{14} \text{ cm}^{-3}$ injection for $11.2 \Omega \text{ cm}$ Cz silicon samples being a factor of >4 higher than in other studies of similar resistivity Cz silicon samples^[29,32] which show the lifetime to plateau at around 1 ms. Using more resistive Ga-doped substrates (e.g., up to $2\text{--}3 \Omega \text{ cm}$) could therefore provide a route to higher cell efficiencies, but this would depend on the balance between enhanced lifetime and reductions in cell performance at higher substrate resistivities, which can be determined by simulation.^[38] Second, all effective lifetimes reported for Ga-doped silicon lie well below the intrinsic limit, aside from those reported by Cizek et al., who demonstrate the potential of gallium-doped silicon when grown-in defects are significantly reduced in FZ silicon (e.g., swirl-like defects).^[30] Recent analysis of lifetime in indium-doped silicon^[39] has found recombination linked to unionized indium, and although gallium's energy level at $E_V + 0.073 \text{ eV}$ is less deep than that of indium ($E_V + 0.156 \text{ eV}$), it is deeper than that of boron ($E_V + 0.044 \text{ eV}$), and this possibility should be explored further. Therefore, given the recent new dominance of gallium-doped wafers, research to understand the lifetime limits of this material, building on that shown in Figure 2a, could enable higher solar cell efficiencies to be achieved.

2.2. Anomalous LID Behavior in Ga-Doped PERC Cells

Having assessed the lifetime potential of gallium-doped silicon, and identified where the lifetime can be improved, we now assess the stability of gallium-doped PERC solar cells when subject to extended illumination at elevated temperature, as it has been documented that this material does not undergo any significant levels of degradation under illumination at room temperature.^[5,6]

As reported in our previous study,^[13] a 300°C dark anneal triggers degradation in Ga-doped PERC cells when illuminated at 1 Sun equivalent and 75°C for $\approx 1000 \text{ h}$. We denote this data set as Batch 1, and results are shown in Figure 3a. The normalized photoluminescence (PL) intensity goes down to about 80% of the initial value, which is considerably less degradation than in B-doped cells, where the signal can go down to about 60–40% of the initial value. Stripping the cells after degradation and passivating the stripped cells with a temporary room temperature method,^[40] revealed the deterioration was due to a reduction in bulk excess carrier lifetime. In contrast, Batch 1 cells which did not undergo a dark anneal showed no, or very little, sign of degradation when subjected to the same illumination conditions. This was an encouraging result which implied that “as-processed” cells would not degrade when deployed in the field.

Importantly, results from our most recent batch of Ga PERC cells (Batch 2), have revealed the opposite trend to that observed for Batch 1 cells, as shown in Figure 3b. In this case, stable cell performance under 1 Sun illumination and 75°C occurs after the

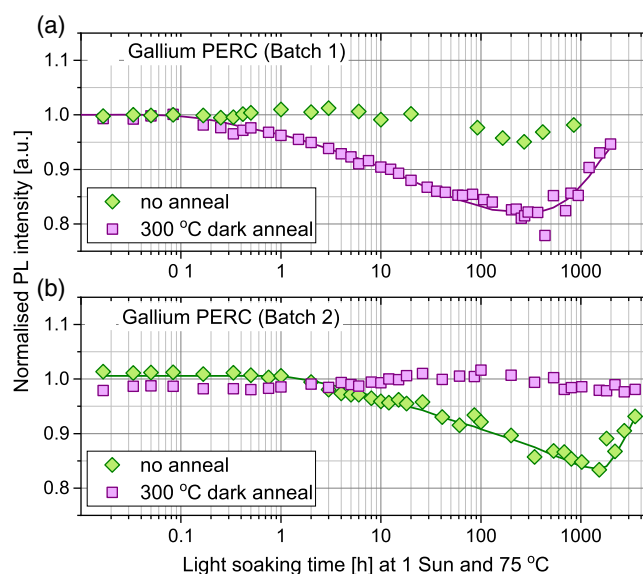


Figure 3. Normalized PL intensity from the proxy method versus light-soaking time at 1 Sun equivalent and 75°C for PERC devices. Data in a) from Batch 1 are from our previous study^[13] and data in b) come from Batch 2 which had a slightly different cell architecture (e.g., rear metallization and contacting patterns). The resistivity of the base Ga silicon material for Batches 1 and 2 are 1.6 and $0.7 \Omega \text{ cm}$, respectively. The purple squares and green diamonds correspond to PERC cells with and without a 300°C dark anneal for 30 min, respectively. Solid lines are guides to the eye.

300°C dark anneal, while cells undergo a significant level of degradation if no dark anneal is performed. These experiments were repeated on additional cell samples to ensure their reproducibility. Thus, the batches behave completely differently from an LID perspective.

We can think of two possible routes of enquiry into the difference. The first is that the variations in manufacturing processes between Batch 1 and Batch 2 cells have impacted on the degradation behavior, and the second is that the degradation is controlled by a variable material property of the wafers. In terms of cell process differences, the rear metallization pattern has undergone a design change in the layout of the contact geometry. This relatively small design change required a different, albeit similar, firing profile. It is well known that the slightest change in firing conditions can substantially influence the subsequent degradation behavior under illumination, as demonstrated for boron-doped cells and test structures.^[41–46] In terms of materials properties, the most obvious difference is that the resistivity of the base Ga material has changed from $\approx 1.5 \Omega \text{ cm}$ for Batch 1 to $\approx 0.7 \Omega \text{ cm}$ for Batch 2, so the differing levels of Ga could play a role in the degradation process. A source of variation could originate from other differences in the wafers, and each wafer could contain a differing level of grown-in intrinsic point defects (vacancies and interstitials), light impurities (e.g., oxygen, nitrogen, and carbon), and metallic impurities, which could vary from one ingot to another, or even from one end of a given ingot to the other. There are plenty of known examples in which intrinsic point defects, light impurities and metallic impurities can

contribute to degradation of carrier lifetime, which we have shown to be occurring by carrying out measurements on stripped PERC cells in our previous study.^[13]

In summary, the reasons for the differences in behavior between Batch 1 and 2 cells fabricated around a year apart are not clear. Noting that we have observed radical differences in LID behavior in solar cells produced by the same manufacturer, it is highly likely that cells from other manufacturers will also encounter variable degradation behavior when manufacturing modifications are made, and thus it is important that the source of degradation is identified.

2.3. Impact of Cell Stabilization Processes

Over the past few years, there have been substantial improvements in stabilizing boron-doped silicon solar cells by subjecting the finished cells to a stabilization treatment, e.g., by annealing finished cells while applying a very large current.^[25,47] In our previous study,^[13] we demonstrated the benefit of such stabilization treatments on B-doped PERC solar cells, finding that stabilized cells subject to 1 Sun equivalent treatment at 75 °C for ≈ 1000 h actually resulted in improved cell performance for stabilized cells, indicating the cells had not been fully regenerated during the BO-stabilization process. In contrast, a boron-doped PERC cell which had been destabilized, e.g., by a 300 °C dark anneal, showed significant degradation when subject to the same illumination conditions, thereby visually demonstrating the significance of the stabilization treatment. Since these experiments were conducted, the PV industry has seen a rapid switch from B-doped silicon to Ga silicon, a move primarily driven by improved device stability (without stabilization processes) and cell efficiency, the latter benefiting from the higher lifetimes achieved using Ga silicon material.^[4] Nevertheless, given the PV industry have built up the capabilities to perform stabilization treatments on B-doped silicon, it is important to assess whether they may be needed for Ga-doped silicon or whether they can be omitted altogether. Therefore, in this work, we investigate the impact of carrying out a boron–oxygen style stabilization treatment on Ga PERC cells from Batch 2—as Ga-doped Cz contains equivalent levels of oxygen to B-doped silicon—and directly compare them to identically processed cells which have not undergone the stabilization treatment. The results are shown in **Figure 4**.

Figure 4 shows the normalized PL intensity versus light-soaking time for Ga PERC solar cells which have (blue circles) and have not (orange squares) undergone a boron–oxygen style stabilization process. It is clear that the “stabilization” process has not had an impact on the degradation characteristics of the Ga PERC cells investigated, evident by the two data sets (with and without stabilization) following near identical trends. In contrast, near complete stability occurs once the Ga PERC cells have been subjected to a 300 °C dark anneal, regardless of whether the cells had been subject to a “stabilization” treatment or not, which is an interesting observation, because such anneals traditionally destabilize the cells by reactivation of bulk defects in the silicon material.^[19,48] Thus, the only resemblance in the LID characteristics of the data shown in Figure 4, to that observed in other studies, is the trend, e.g., degradation followed by a recovery. It is therefore difficult to ascertain whether the

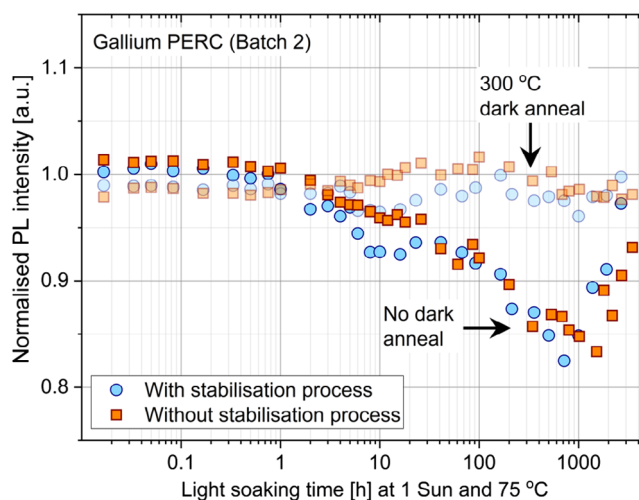


Figure 4. Normalized PL intensity from the proxy method versus light-soaking time (1 Sun equivalent at 75 °C) for Ga-doped PERC solar cells from Batch 2 (0.7 Ωcm substrates) which have and have not undergone a boron–oxygen style stabilization process. Sister samples were either subjected to no dark anneal (solid symbols) or to a 300 °C dark anneal for 30 min prior to light soaking (faded symbols).

defect causing this degradation and recovery in Ga-doped PERC is similar to that observed in nonstabilized B-doped PERC cells, e.g., boron–oxygen complexes and/or hydrogen-related defects. Nevertheless, Figure 3a shows that Ga PERC cells can be manufactured in a way that mitigates LID without additional stabilization processes. Knowing why the cells degrade in some cases and not others would be hugely beneficial in manufacturing *p*-type cells with complete self-stability.

2.4. Unintentional Boron Contamination of Ga PERC Cells

Our investigation of LID in Ga-doped PERC solar cells has thus far been mainly observational. To gain possible insight into the potential origin of degradation, we have taken Ga-doped PERC cells which showed differing levels of degradation upon extended illumination at 1 Sun equivalent and 75 °C, and have stripped them of their metal and dielectric coatings, and etched the near-surface region using methods described in Experimental Section. We have then carried out four-point probe (4pp) measurements to determine the resistivity, and secondary-ion mass spectrometry (SIMS) measurements (on selected stripped cell materials) to establish the presence of unintentional boron doping. The gallium doping level was also measured by SIMS (**Table 1**) and gave similar values to those implied by 4pp measurements.

Table 1. SIMS measurements of gallium and boron concentrations in the Cz silicon wafers from two different Ga PERC silicon solar cells stripped of their metallization, dielectrics, and diffusions. The detection limit was $5 \times 10^{12} \text{cm}^{-3}$.

Material	Gallium concentration [cm^{-3}]	Boron concentration [cm^{-3}]
Batch 1	1.0×10^{16}	8.2×10^{13}
Batch 2	2.4×10^{16}	3.7×10^{13}

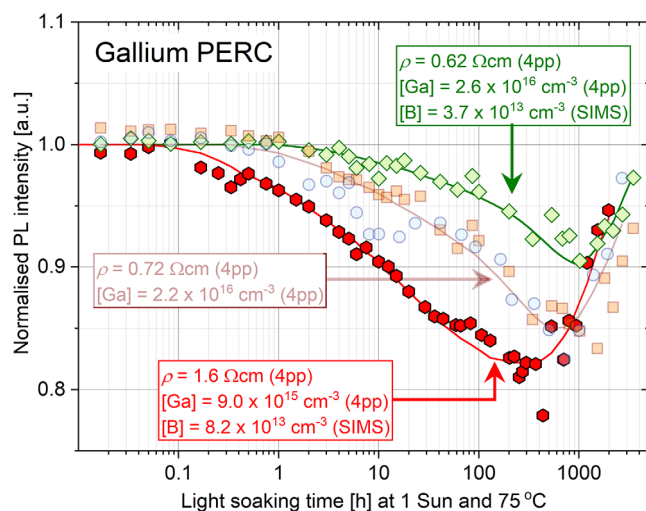


Figure 5. Normalized PL intensity from the proxy method versus light-soaking time (1 Sun equivalent at 75 °C), for Ga PERC devices featuring different degrees of degradation. Red hexagons arise from cells from Batch 1 and green diamonds from cells from Batch 2. The faded orange squares and blue circles correspond to the data shown in Figure 4, and thus are also from Batch 2 cells. Solid lines are guides to the eye. Four-point probe (4pp) measurements were used to determine the resistivity on cells which had been stripped back to the silicon substrate, whereas the B concentration was determined by SIMS measurements.

From Table 1 and **Figure 5**, it is evident that both Ga materials which underwent SIMS measurements, showed unintentional boron doping, albeit in low concentrations, which could arise from a number of different sources, examples being the silicon feedstock, gallium doping source, crucible, and perhaps even the Al pastes (containing B) used for the back surface field. The latter however, is not expected to drive boron deep into the bulk of the silicon material, and thus is an unlikely source of degradation observed in Ga PERC cells. With knowledge of the unintentional boron concentration, and the level of degradation observed in each cell, there does appear to be a correlation, where we observe a doubling in the level of degradation for the sample with twice as much unintentional boron doping. However, our data do not yield sufficient evidence to conclude that a boron-related defect is causing varying levels of LID in Ga PERC, rather it merely serves as a possibility, and one which researchers should not overlook when examining Ga material, or perhaps even *n*-type silicon PV materials.

An alternative interpretation of the data shown in Figure 5, is that the level of degradation is influenced by the Ga doping level. For example, the highest level of degradation is observed for the lowest-doped Ga material and vice versa. We also note that the onset of maximum degradation also appears to scale with doping concentration, with the highest-doped Ga material taking ≈ 1000 h and the lowest taking ≈ 700 h. While this interpretation seems counterintuitive, recent work by Kwapił et al., has demonstrated that the level of LID at 75 °C in Ga-doped silicon material is injection-level dependent.^[22] Thus, as we have not changed the illumination conditions (1 Sun equivalent) for experiments on the differently doped materials, means the level of carrier

injection during light soaking differs. For example, a 0.6 Ω cm Ga silicon wafer will undergo lower carrier injection at 1 Sun equivalent illumination if the effective lifetime is lower than for a 1.6 Ω cm Ga silicon wafer. Therefore, we cannot rule out the impact of different injection levels as a cause for the varying levels of degradation shown in Figure 5. Considering this, and noting the presence of unintentional boron doping, it is not yet possible to rule out either element as a possible source for LID observed in Ga silicon material.

3. Conclusions

In this work, we investigated the lifetime potential of gallium-doped silicon wafers and demonstrated that “as-received” Ga-doped wafers had comparable lifetimes to treated (gettered and stabilized) B-doped wafers, meaning Ga-doped silicon has more potential to achieve higher lifetimes once gettered and subjected to fast firing, as commonly carried out in solar cell fabrication lines. We analyzed the injection-dependent lifetime of our Ga-doped silicon, and inferred the presence of iron, and a secondary unknown defect, which could limit the cell efficiency through a reduction in V_{mpp} if not mitigated. By comparing our lifetime data to those in the literature, it appears that Ga-doped silicon usually suffers from recombination associated with an unknown defect. However, it is difficult to ascertain whether this is due to the Ga dopant itself, or another grown-in defect formed during crystal growth.

Not only the lifetime itself, but also its stability is important to PERC solar cells. We therefore subjected the cells to extended illumination at 100 mW cm⁻² and elevated temperature. It was discovered that Ga-based PERC cells from the same manufacturer, but different batches, provide contradictory LID behavior, whereby LID was triggered by a 300 °C dark anneal post cell fabrication for Batch 1, and vice versa for Batch 2, with the latter being far more alarming. We investigated the impact of carrying out a boron–oxygen style stabilization process on Batch 2 Ga PERC cells, and demonstrated, at least for this batch, the stabilization treatment had no effect, and the cells degraded in a near identical fashion to sister cells which did not undergo the post cell fabrication treatment. Through SIMS measurements, it was discovered that unintentional boron doping was present in stripped and etched Ga-doped PERC cell substrates, whereby the degradation level in each cell was found to be dependent on the boron and gallium concentrations. However, our studies to date are not detailed enough to confirm the involvement of unintentional boron doping as the main source of degradation, or its counterintuitive dependence on gallium concentration, rather they serve as a guidance for further research on Ga PERC solar cell materials. Nevertheless, despite drawing some attention to lifetime and stabilization issues in Ga-doped silicon, it is still important to note that without any extensive treatments, Ga-doped silicon has better intrinsic stability than B-doped silicon making it an attractive option for mass-market production.

4. Experimental Section

For the lifetime part of the study, (100)-orientation 156 × 156 mm² gallium-doped Cz silicon wafers with different resistivities (0.3–11.2 Ω cm)

were used. Resistivity values were averages across the samples. Samples with the size of $5 \times 5 \text{ cm}^2$ were cleaved from the 170–180 μm thick wafers and each was subjected to a careful surface passivation procedure with aluminum oxide grown by ALD. Before deposition, each sample was subjected to a careful surface preparation procedure which included i) a standard clean 1 (SC1) process comprising H_2O , H_2O_2 (30%), NH_4OH (30%) (5:1:1) at $\approx 80^\circ\text{C}$ for 10 min; ii) a 1% HF dip; iii) a 25% TMAH etch for 10 min at $\approx 80^\circ\text{C}$; iv) a 1% HF dip; v) an SC2 clean for 10 min at $\approx 80^\circ\text{C}$; and then vi) a dip in HF (2%). After the final step, the sample was pulled dry from the HF without being subjected to a deionized water rinse. ALD was carried out using a Veeco Fiji G2 system featuring an external load lock. Aluminum oxide was deposited at 200°C using a plasma O_2 source and a trimethylaluminum precursor for 200 cycles to give films $\approx 20 \text{ nm}$ thick, with the process repeated for the second side of the sample. To activate the passivation, a postdeposition anneal in air was carried out in a quartz tube furnace at $460 \pm 10^\circ\text{C}$ for 30 min. We have previously shown that this process flow results in a surface recombination velocity $< 0.5 \text{ cm s}^{-1}$.^[49] Lifetimes were measured at room temperature using a Sinton WCT-120 lifetime tester, which was calibrated using a recently proposed method.^[50] Unless otherwise stated, lifetime measurements were taken directly after illuminating the samples for 20 s at 100 mW cm^{-2} to minimize the impact of iron–gallium recombination centers.^[9–11]

For the cell part of the study, we investigate PERC devices produced industrially by Trina SKL from Ga-doped (100)-orientation Cz silicon substrates. Cells were from two batches. Batch 1 cells are those from our previous publication^[13] which had an average batch efficiency of 22.1–22.2% (individual cells were not measured) and a substrate resistivity of $1.5 \Omega \text{ cm}$. Batch 2 cells were fabricated about a year later using an incrementally improved cell design and process sequence using $0.7 \Omega \text{ cm}$ resistivity substrates resulting in an efficiency of around 22.8%. Some Batch 2 cells were subjected to a postproduction “stabilization” process of the kind typically used to mitigate boron–oxygen-related LID. This involved exposing a large stack of finished cells with such a high current density that it causes a rather uncontrolled elevated temperature anneal, as is typically done in industry. The properties of the cells from Batch 2 used for the experiments in this article are shown in **Table 2**, and the parameters are very similar with and without the “stabilization” process. Cells were cleaved into $5 \times 5 \text{ cm}^2$ samples for light-soaking experiments. These samples were placed on hotplates to maintain a 75°C sample temperature while being illuminated with a halogen lamp with an approximate power density of 1000 W m^{-2} (1 Sun equivalent). The cell properties were monitored with a nondestructive PL proxy method described previously.^[13] This involves monitoring the PL signal from the same $2 \times 2 \text{ cm}^2$ region as a function of light-soaking time, and the method gives a noninvasive measure of cell performance without risking damage to the cell contacts and surfaces.

SIMS was carried out on selected samples to measure bulk dopant concentrations. Completed PERC cells were stripped down to the base silicon substrate by removal of front and rear metal contacts, dielectrics, and diffused regions. The procedure to strip the cells was as follows i) An aqua regia metal etch consisting of HCl (37%) and HNO_3 (69.5%) mixed in the ratio 3:1. This was left to react for 15 min before adding the samples, which were etched for 15 min. ii) Immersion in 50% HF for 10 min. iii) SC1 clean followed by a dip in 1% HF. iv) A silicon etch in a solution of HF (50%) and HNO_3 (69.5%) in the ratio 1:10 for 3 min. v) A dip in 1% HF for 1 min, followed by a deionized H_2O rinse. It is estimated that $5 \mu\text{m}$ of material was removed from each surface as part of the stripping process,

Table 2. Measured cell properties including open-circuit voltage (V_{OC}), short-circuit current density (J_{SC}), and FF for the Ga PERC cells from Batch 2 subjected to light-soaking experiments in this article.

Cell	V_{OC} [mV]	J_{SC} [mA cm^{-2}]	FF [%]	Efficiency [%]
Without stabilization	685	40.9	81.3	22.8
With stabilization	685	40.8	81.4	22.8

ensuring the measurement to reflect bulk wafer concentrations. SIMS experiments were conducted by Eurofins EAG Materials Science (Sunnyvale, CA, USA) and the detection limit for both boron and gallium was $5 \times 10^{12} \text{ cm}^{-3}$. The values reported are an average over $> 1.5 \mu\text{m}$ of depth near the new surface. The resistivity of some stripped cells was also measured by 4pp.

Acknowledgements

Work at Warwick was supported by the EPSRC SuperSilicon PV project (EP/M024911/1), an EPSRC First Grant (EP/J01768X/2), and the International and Industrial Engagement Fund of the EPSRC Supergen Solar Network+ (EP/S000763/1). The authors at Fraunhofer ISE and University of Freiburg acknowledge funding from BMWi under contract numbers 0324204A and 0324204C.

Conflict of Interest

The authors declare no conflict of interest.

Data Availability Statement

Data openly available in a public repository that does not issue DOIs, <https://wrap.warwick.ac.uk/148701>.

Keywords

gallium, lifetime, light-induced degradation, passivated emitter and rear, silicon

Received: November 27, 2020

Revised: February 17, 2021

Published online: March 1, 2021

- [1] T. Niewelt, J. Schön, W. Warta, S. W. Glunz, M. C. Schubert, *IEEE J. Photovolt.* **2017**, *7*, 383.
- [2] A. Herguth, G. Hahn, *J. Appl. Phys.* **2010**, *108*, 114509.
- [3] B. Hallam, A. Herguth, P. Hamer, N. Nampalli, S. Wilking, M. Abbott, S. Wenham, G. Hahn, *Appl. Sci.* **2018**, *8*, 10.
- [4] P. P. Altermatt, Y. Yang, Y. Chen, X. Zhang, D. Chen, G. Xu, Z. Feng, *37th European Photovoltaic Solar Energy Conference*, **2020**, p. 1999, <https://doi.org/10.4229/EUPVSEC20202020-7CP.1.2>.
- [5] S. W. Glunz, S. Rein, J. Knobloch, W. Wettling, T. Abe, *Progr. Photovolt. Res. Appl.* **1999**, *7*, 463.
- [6] V. Meemongkolkiat, K. Nakayashiki, A. Rohatgi, G. Crabtree, J. Nickerson, T. L. Jester, *Progr. Photovolt. Res. Appl.* **2006**, *14*, 125.
- [7] J. Schmidt, D. Macdonald, *J. Appl. Phys.* **2005**, *97*, 113712.
- [8] Y. Yoon, Y. Yan, N. P. Ostrom, J. Kim, G. Rozgonyi, *Appl. Phys. Lett.* **2012**, *101*, 222107.
- [9] T. U. Nærlund, S. Bernardini, H. Haug, S. Grini, L. Vines, N. Stoddard, M. Bertoni, *J. Appl. Phys.* **2017**, *122*, 085703.
- [10] R. Post, T. Niewelt, J. Schön, F. Schindler, M. C. Schubert, *Phys. Status Solidi A* **2019**, *216*, 1800655.
- [11] R. Post, T. Niewelt, W. Yang, D. Macdonald, W. Kwapil, M. C. Schubert, *AIP Conf. Proc.* **2019**, *2147*, 020012.
- [12] J. Lindroos, M. Yli-Koski, A. Haarhiltunen, M. C. Schubert, H. Savin, *Phys. Status Solidi RRL* **2013**, *7*, 262.
- [13] N. E. Grant, J. R. Scowcroft, A. I. Pointon, M. Al-Amin, P. P. Altermatt, J. D. Murphy, *Sol. Energy Mater. Sol. Cells* **2020**, *206*, 110299.

- [14] D. Chen, M. V. Contreras, A. Ciesla, P. Hamer, B. Hallam, M. Abbott, C. Chan, *Progr. Photovolt. Res. Appl.* **2021**, <https://doi.org/10.1002/pip.3362>.
- [15] T. Niewelt, M. Selinger, N. E. Grant, W. M. Kwapil, J. D. Murphy, M. C. Schubert, *J. Appl. Phys.* **2017**, *121*, 185702.
- [16] F. Kersten, P. Engelhart, H.-C. Ploigt, A. Stekolnikov, T. Lindner, F. Stenzel, M. Bartzsch, A. Szpeth, K. Petter, J. Heitmann, J. W. Müller, *Sol. Energy Mater. Sol. Cells* **2015**, *142*, 83.
- [17] F. Fertig, K. Krauß, S. Rein, *Phys. Status Solidi RRL* **2015**, *9*, 41.
- [18] A. Zuschlag, D. Skorka, G. Hahn, *Progr. Photovolt. Res. Appl.* **2017**, *25*, 545.
- [19] D. Chen, M. Kim, B. V. Stefani, B. J. Hallam, M. D. Abbott, C. E. Chan, R. Chen, D. N. R. Payne, N. Nampalli, A. Ciesla, T. H. Fung, K. Kim, S. R. Wenham, *Sol. Energy Mater. Sol. Cells* **2017**, *172*, 293.
- [20] D. Chen, P. G. Hamer, M. Kim, T. H. Fung, G. Bourret-Sicotte, S. Liu, C. E. Chan, A. Ciesla, R. Chen, M. D. Abbott, B. J. Hallam, S. R. Wenham, *Sol. Energy Mater. Sol. Cells* **2018**, *185*, 174.
- [21] B. Wright, C. Madumelu, A. Soeriyadi, M. Wright, B. Hallam, *Solar RRL* **2020**, *4*, 2000214.
- [22] W. Kwapil, J. Dalke, T. Niewelt, M. C. Schubert, *37th European Photovoltaic Solar Energy Conf.*, **2020**, p. 152, <https://doi.org/10.4229/EUPVSEC20202020-2AO.5.3>.
- [23] G. Fischer, F. Wolny, H. Neuhaus, M. Müller, *37th European Photovoltaic Solar Energy Conf.*, **2020**, p. 238, <https://doi.org/10.4229/EUPVSEC20202020-2CO.13.2>.
- [24] K. Bothe, R. Sinton, J. Schmidt, *Progr. Photovolt. Res. Appl.* **2005**, *13*, 287.
- [25] D. C. Walter, B. Lim, J. Schmidt, *Progr. Photovolt. Res. Appl.* **2016**, *24*, 920.
- [26] B. Hoex, S. B. S. Heil, E. Langereis, M. C. M. van de Sanden, W. M. M. Kessels, *Appl. Phys. Lett.* **2006**, *89*, 042112.
- [27] A. Richter, S. W. Glunz, F. Werner, J. Schmidt, A. Cuevas, *Phys. Rev. B* **2012**, *86*, 165202.
- [28] F. E. Rougieux, C. Sun, D. Macdonald, *Sol. Energy Mater. Sol. Cells* **2018**, *187*, 263.
- [29] S. K. Pang, A. Rohatgi, T. F. Cizek, *Conf. Record of the Twentieth IEEE Photovoltaic Specialists Conf.*, IEEE, Piscataway, NJ **1988**, p. 435, <https://doi.org/10.1109/PVSC.1988.105738>.
- [30] T. F. Cizek, T. Wang, T. Schuyler, A. Rohatgi, *J. Electrochem. Soc.* **1989**, *136*, 230.
- [31] A. Metz, T. Abe, R. Hezel, *16th European Photovoltaic Solar Energy Conf.*, Glasgow, UK **2000**, p. 1189.
- [32] S. W. Glunz, S. Rein, J. Knobloch, *16th European Photovoltaic Solar Energy Conf.*, Glasgow, UK **2000**, p. 1070.
- [33] G. Crabtree, T. L. Jester, C. Fredric, J. Nickerson, V. Meemongkolkiat, A. Rohatgi, *31st IEEE Photovoltaic Specialists Conf.*, IEEE, Buena Vista, FL, USA **2005**, p. 935, <https://doi.org/10.1109/PVSC.2005.1488285>.
- [34] B. Lim, A. Merkle, R. Peibst, T. Dullweber, Y. Wang, R. Zhou, *35th European Photovoltaic Solar Energy Conf.*, Brussels, Belgium **2018**, p. 359, <https://doi.org/10.4229/35thEUPVSEC20182018-2BO.3.2>.
- [35] A. Fell, P. P. Altermatt, *IEEE J. Photovolt.* **2018**, *8*, 1443.
- [36] C. Messmer, A. Fell, F. Feldmann, N. Wöhrle, J. Schön, M. Hermle, *IEEE J. Photovolt.* **2020**, *10*, 335.
- [37] N. E. Grant, J. D. Murphy, *Phys. Status Solidi RRL* **2017**, *11*, 1700243.
- [38] F. Schindler, B. Michl, P. Krenckel, S. Riepe, J. Benick, R. Müller, A. Richter, S. W. Glunz, M. C. Schubert, *Sol. Energy Mater. Sol. Cells* **2017**, *171*, 180.
- [39] J. D. Murphy, A. I. Pointon, N. E. Grant, V. A. Shah, M. Myronov, V. V. Voronkov, R. J. Falster, *Progr. Photovolt. Res. Appl.* **2019**, *27*, 844.
- [40] A. I. Pointon, N. E. Grant, E. C. Wheeler-Jones, P. P. Altermatt, J. D. Murphy, *Sol. Energy Mater. Sol. Cells* **2018**, *183*, 164.
- [41] S. Wilking, A. Herguth, G. Hahn, *J. Appl. Phys.* **2013**, *113*, 194503.
- [42] D. C. Walter, B. Lim, K. Bothe, V. V. Voronkov, R. Falster, J. Schmidt, *Appl. Phys. Lett.* **2014**, *104*, 042111.
- [43] R. Eberle, W. Kwapil, F. Schindler, M. C. Schubert, S. W. Glunz, *Phys. Status Solidi RRL* **2016**, *10*, 861.
- [44] R. Sharma, A. G. Aberle, J. B. Li, *Sol. RRL* **2018**, *2*, 1800070.
- [45] C. Sen, M. Kim, D. Chen, U. Varshney, S. Liu, A. Samadi, A. Ciesla, S. R. Wenham, C. E. Chan, C. Chong, M. D. Abbott, B. J. Hallam, *IEEE J. Photovolt.* **2019**, *9*, 40.
- [46] B. J. Hallam, P. G. Hamer, A. M. Ciesla, C. E. Chan, B. V. Stefani, S. Wenham, *Progr. Photovolt. Res. Appl.* **2020**, *28*, 1217.
- [47] I. L. Repins, F. Kersten, B. Hallam, K. VanSant, M. B. Koentopp, *Sol. Energy* **2020**, *208*, 894.
- [48] S. Wilking, C. Beckh, S. Ebert, A. Herguth, G. Hahn, *Sol. Energy Mater. Sol. Cells* **2014**, *131*, 2.
- [49] N. E. Grant, A. I. Pointon, R. Jefferies, D. Hiller, Y. Han, R. Beanland, J. D. Murphy, *Nanoscale* **2020**, *12*, 17332.
- [50] L. E. Black, D. H. Macdonald, *IEEE J. Photovolt.* **2019**, *9*, 1563.